REVIEW

Self-assembly of organic luminophores with gelation-enhanced emission characteristics

Zujin Zhao,[a] Jacky W. Y. Lam[b] and Ben Zhong Tang*[bc]

Fluorescent self-assembled organogels are interesting supramolecular soft materials with polymer-like structures and have received particular attention due to their fascinating properties and promising practical applications. However, most planar π-conjugated gelators are highly emissive in the solution state but become weak emitters when self-assembled. Recently, a novel phenomenon of aggregation-induced emission (AIE) has drawn increasing research interest and has been the subject of numerous investigations. This intriguing finding paves a new way for creating fluorescent organogels by utilizing gelators with AIE characteristics. This review focuses on the recent advances in fluorescent organogels with gelation-enhanced emission features. Various kinds of low molecular weight gelators consisting of typical AIE luminogens, conventional planar chromophores, and photoactive molecules are introduced and the mechanisms for the emission enhancement are discussed.

1 Introduction

Self-assembled supramolecular gels are a new class of important soft materials and their fabrication has emerged as a hot research topic in the past decade owing to their novel material properties and potential applications.[1–10] These viscoelastic gels are composed of a small amount of gelators in a large pool of solvents, typically with a concentration of 1% by weight. The gelation process is generally believed to involve first the self-assembly of gelators into one-dimensional (1D) fibrous nanomaterials driven by multiple, weak non-covalent interactions such as hydrogen bonding, π-stacking interactions, dipole–dipole interactions, van der Waals forces, *etc.* These nanofibers then tangle together to form a three-dimensional (3D) network, which endows the gels with strong ability to immobilize the solvent molecules and hence interesting properties that are in between those of solids and liquids. Such supramolecular gels are of particular interest because of their unique attributes of non-polymeric nature and sensitive response to external stimulation, such as temperature,[11–13] light,[14,15] protons,[16,17] metal ions,[18,19] *etc.* Thereby, supramolecular gels are considered as

[a]*College of Material, Chemistry and Chemical Engineering, Hangzhou Normal University, Hangzhou 310036, China*

[b]*Department of Chemistry, Institute of Molecular Functional Materials, State Key Laboratory of Molecular Neuroscience and Institute for Advanced Study, The Hong Kong University of Science & Technology (HKUST), Clear Water Bay, Kowloon, Hong Kong, China. E-mail: tangbenz@ust.hk*

[c]*Guangdong Innovative Research Team, SCUT-HKUST Joint Research Laboratory, State Key Laboratory of Luminescent Materials and Devices, South China University of Technology (SCUT), Guangzhou, 510640, China*

Zujin Zhao received his PhD degree from Zhejiang University in 2008. In 2008–2010, he conducted his postdoctoral work under the supervision of Prof. Ben Zhong Tang at HKUST. Since then, he has been an associate professor of chemistry in Hangzhou Normal University. His research focuses on the development of luminescent materials including organic small molecules and conjugated polymers and exploration of their opto-electronic applications.

Jacky W. Y. Lam received his Ph.D. degree from HKUST in 2003 under the supervision of Prof. Tang. In 2003–2007, he carried out his postdoctoral work on novel polymers with linear and hyperbranched structures and advanced functional properties in Tang's group. He is currently a research assistant professor of chemistry at HKUST.

"smart" materials and have found diverse applications in template synthesis,[20,21] drug delivery,[22,23] light harvesting,[24,25] biomimetic systems,[26] electronics,[27,28] etc.

Thanks to the enthusiasm of chemists and materials scientists, a general design principle of gelators has been established. Gelators usually possess several characteristics including strong self-complementary and unidirectional intermolecular interactions to induce 1D self-assembly and abundant weak secondary interactions that enable the 1D nanoaggregates to form cross-linked 3D supramolecular networks. Long flexible alkyl chains and other specific groups such as steroidal groups, urea, amides, nucleobases, surfactants and sugars are found, somewhat unexpectedly, to be beneficial for gelation and consequently have been widely adopted in the design of gelators, for their superability to induce the molecules to form fibrous structures. However, it remains difficult to explicitly predict the gelation phenomenon or perfectly explain the structure–property relationship due to the complex gelator–gelator and gelator–solvent interactions, revealing that the research on supramolecular gels is still in the early stage of its development.

Among various supramolecular gels, fluorescent organogels constructed from π-conjugated low molecular weight gelators[4,5,28–32] have attracted intense interest and are extensively studied due to their academic importance and distinctive advantages such as diversity, flexibility and promising applications in optoelectronics,[33–35] fluorescence sensors,[36–41] etc. However, most π-conjugated molecules suffer from emission quenching in the condensed phase although they emit efficiently in the solution state. The severe intermolecular interactions that are conducive to self-organization generally consume the excited state energy and thus debilitate the light emission of the self-assembled nanomaterials.[42–44] Therefore, how to solve the emission quenching problem becomes a complex task and, in most cases, is a dilemma. To achieve a substantial breakthrough, development of tailored π-conjugated gelators with efficient emissions in the aggregated state is of decisive significance. In particular, it will be nice, if a system

can be developed, in which the light emission of the gelator is enhanced, rather than quenched by gelation.[45–48] This will make life much easier because the gelation now works to our benefit: no hard work will need to be done to artificially interrupt the very natural process of aggregation.

In 2001, Tang and co-workers observed that a group of silole derivatives are non-fluorescent in the solution state but become highly emissive in the aggregated state (as nanoparticle suspensions in poor solvents or as thin solid films).[49] The term "aggregation-induced emission" (AIE) was coined for this unusual phenomenon because the non-emissive molecules are induced to emit by aggregate formation. The abnormal AIE effect is the exact opposite of the aggregation-caused quenching effect observed in most conventional chromophores. The phenomenon is of academic value because it challenges our current understanding of photoluminescence (PL) processes.[50–54] Deciphering the causes and mechanisms of the AIE phenomenon helps to spawn new photophysical theories and technological innovations. The phenomenon also has practical implications as it permits the use of dye solutions with any concentration for sensing applications and enables the development of "turn on" or "light up" fluorescent sensors by taking advantage of luminogenic aggregation.[55] In addition, recent studies have demonstrated that the nanoparticles of AIE luminogens are super probes for *in vitro* and *in vivo* imaging[56] and their films with colors covered from blue to red show outstanding electroluminescence properties in non-doped organic light-emitting diodes,[57,58] revealing that they are promising solid-state light emitters for panel displays.

Attracted by the intriguing photophysical properties and fascinating perspectives, more and more research groups have embarked on the area of AIE research and have done a large amount of outstanding work on nanostructured materials with AIE features. Various nanofibers,[48,59,60] nanorings,[61] nanotubes,[62] and nanospheres[63,64] have been prepared from AIE luminogens. Recently, the AIE effect has been studied in organogel systems.[47] Many organogelators show enhanced emissions in the gel state or gelation-enhanced emission characteristics. In this review, we elaborate the recent progress in this rapidly evolving area and focus on representative organogels consisting of not only typical AIE luminogens such as tetraphenylethene (TPE), silole and cyanostilbene derivatives, but also non-classical AIE luminogens such as carbazole-based dendrimers, 1,3,4-oxadiazole derivatives and chromophores with excited-state intramolecular proton transfer (ESIPT) features. The structure–property relationships of these supramolecular organogels and the mechanism for the gelation-enhanced emission are discussed.

2 Organogels with typical AIE-active gelators

2.1 Gelators carrying tetraphenylethene luminogens

TPE is an archetypal luminogen with intriguing AIE effects. It is almost non-fluorescent in solution but emits efficiently when aggregated as nanoparticles in a poor solvent or fabricated as a film in the solid state. Thanks to its simple molecular structure,
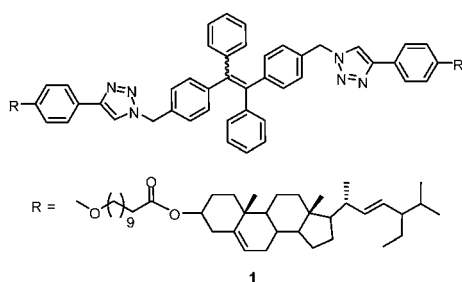
Ben Zhong Tang received his Ph.D. degree from Kyoto University in 1988. He conducted his postdoctoral work at the University of Toronto and worked as a senior scientist in Neos Co., Ltd. He joined HKUST in 1994 and was promoted to Chair Professor in 2008. He is interested in the creation of new molecules with novel structures and unique properties. He received a Natural Science Award from Chinese Government in 2007 and was elected to Chinese Academy of Sciences in 2009. He is serving as News Contributor to Noteworthy Chemistry (ACS), Editor-in-Chief of Polymer Chemistry Series (RSC), and Associate Editor of Polymer Chemistry (RSC).
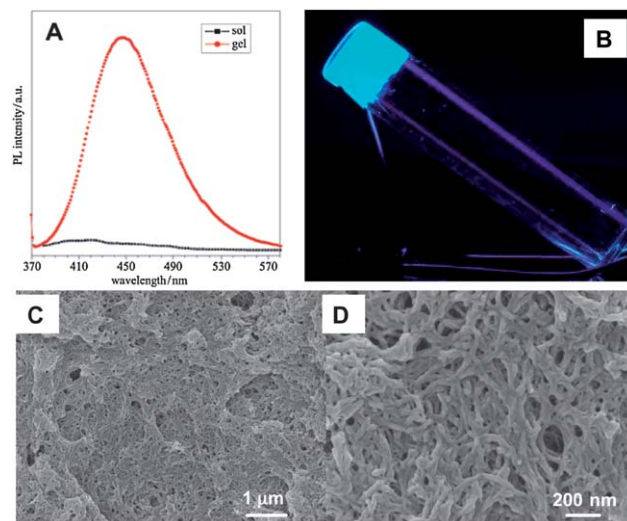
through facile chemical modification, plenty of functional TPE derivatives have been developed and have found an array of high-technological applications as fluorescent chemo-sensors,[55,65,66] bioprobes,[67,68] optoelectronic materials,[58,69,70] *etc.* Whereas pristine TPE can only grow into bulky crystals, its derivatives have shown good self-assembly ability even though they possess propeller-like molecular conformations. For example, 1-[4-(1,2,2, triphenylvinyl)phenyl]-1,2,2-triphenyle-thene, a luminogen prepared by connecting two TPE units through a covalent single bond, can self-assemble into crystal-line nanofibers[71] and nanotubes[62] with a high PL efficiency up to unity.

Recently, Tang and co-workers developed an AIE-active gelator **1** (Chart 1) by attaching a stigmasterol group to TPE through a "click" reaction.[72] Compared with TPE, **1** possesses a more flexible structure due to the presence of a long alkyl chain in the molecular structure. This luminogen is weakly fluorescent in the solution state but turns out to be highly emissive in the aggregated state, demonstrating a typical AIE characteristic. Luminogen **1** is an excellent gelator and can facilely self-assemble into organogels by gentle heating and subsequent cooling of its methanol solution to room temperature. The formed organogels show much stronger emission than their isolated species in solution, displaying a phenomenon of gelation-enhanced emission (Fig. 1A and B). Morphology investigation by scanning electron microscopy (SEM) shows that the organogels possess a 3D network con-structed from entangled bundles of fibrous aggregates (Fig. 1C and D). The self-assembly of molecules of **1** into a 3D orga-nogel should largely rigidify their molecular conformations and restrict the intramolecular rotation (IMR) of the periph-eral phenyl rings. This blocks the nonradiative relaxation channel and populates excitons that undergo radiative decay, thus making the organogels highly emissive upon photoexci-tation. However, an analogue luminogen without long "soft" decyl spacer exhibits no such property, suggesting that the van der Waals forces between alkyl chains are important for the gel formation.

To evaluate the effect of the flexible spacer on the gelation process, two new gelators **2** and **3** based on TPE and biphenyl were prepared (Chart 2),[73] in which alkyl chains with different lengths were used to connect the two chromophoric units together. Like most luminogens containing TPE units, these molecules show very weak fluorescence in the solution state but emit strong light in the solid state with fluorescence quantum


Fig. 1 (A) PL spectra of hot methanol solution (∼0.5 wt%) and organogel of **1**. (B) Fluorescent image of organogel of **1** formed in methanol (∼0.5 wt%) taken under UV irradiation. (C and D) SEM images of organogels of **1**. Reproduced with permission from ref. 72. Copyright (2010) Springer.

yields (Φ_F) up to unity, revealing their AIE characteristics (Fig. 2). Luminogen **3** can form highly emissive organogels by cooling its THF solution (60 mg mL^{-1}) from 60 to 4 °C. Since the hydrophobic alkyl linker between the TPE and biphenyl units in **2** is much shorter than that of **3**, its gelation capability becomes weaker and it forms gels only at higher concentration (>90 mg mL^{-1}). When the TPE and biphenyl units are linked

2, m = 5
3, m = 10
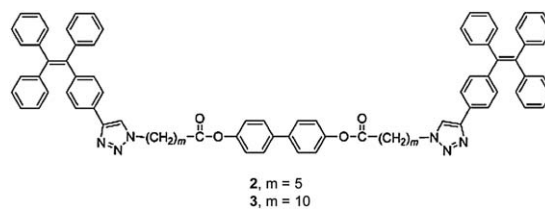
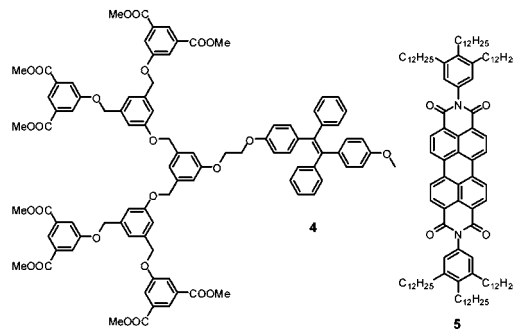**Chart 2** Molecular structures of gelators constructed from TPE and biphenyl.
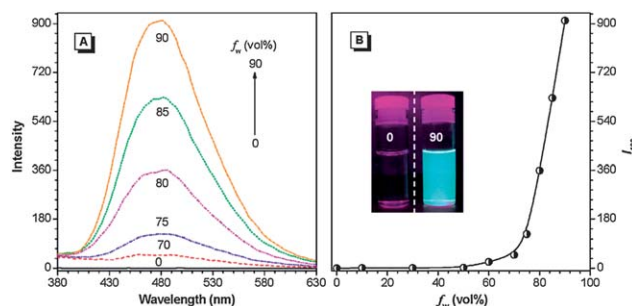
Fig. 2 (A) Emission spectra of **2** in THF and THF–water mixtures with different water fractions (f_w). (B) Plot of the emission peak intensity at 480 nm *versus* water fraction of the aqueous mixture of **2**. Concentration: 20 μM; excitation wave-length: 340 nm. Inset: photographs of **2** in THF–water mixtures with f_w values of 0% and 90% taken under UV illumination. Reproduced with permission from ref. 73. Copyright (2012) The Royal Society of Chemistry.

R =

Chart 1 Molecular structure of TPE-based gelator **1**.

through a rigid triazole ring, the resulting molecule forms no gel at all.

The TEM and SEM images shown in Fig. 3 reveal that the molecules of **3** self-assemble into gels with a fibrous helical nanostructure, which is similar to the fibrous structure of the precipitates formed in THF. Similar morphology was also found in gels of **2**. Such a helical self-assembly behavior accompanying a large emission enhancement is rarely observed and is quite different from those of previously reported TPE derivatives and other AIE luminogens that only form gels with non-helical structures. Visual molecular dynamics simulation results indicate that the molecules of **2** pack tightly through effective intermolecular interactions. The twisted packing motif of the gelators is considered to be responsible for the formation of helical fibrous nanomaterials.[67] Meanwhile, the IMR process is hampered in such a condensed phase, enabling the gelators to fluoresce efficiently.

Besides van der Waals forces between flexible alkyl chains, intermolecular π–π interactions between aromatic rings are also an important driving force for gel formation. Recently, Zhang and co-workers[74] designed and investigated a dendritic gelator **4** by decorating TPE with a benzyl ether-based aromatic hyperbranched dendron (Chart 3). The molecule is capable of forming gels in many aromatic solvents such as benzene and toluene but forms no gels in aliphatic solvents of hexane, cyclohexane, dichloromethane, acetonitrile, ethyl acetate, tetrahydrofuran, methanol and ethanol, suggesting that the multivalent π–π interactions between the dendron molecules


Chart 3 Molecular structures of dendritic gelator **4** and dopant **5**.

and the aromatic solvent molecules are responsible for the gel formation. The xerogel, a dried organogel with unhindered shrinkage, of **4** formed in toluene exhibits a 3D entangled network of long thin nanofibers (Fig. 4), where large fibrous entities with nano-dimensions are made up of entanglement of several twisted small nanofibers.

The organogels of **4** are promising "smart" materials, whose emission color can be modulated by multiple external stimuli. Due to the AIE-active TPE core, **4** is weakly fluorescent in the solution state but its gels emit efficiently. The fluorescence of **4** can be reversibly modulated by solution (sol)–gel transitions driven by alternative heating and cooling processes (Fig. 5). Since the emission spectrum of the organogel overlaps well with the absorption spectrum of perylene diimide **5**, efficient photoinduced energy transfer from **4** to **5** becomes feasible. As a result, the emission color can be tuned readily by varying the doping concentration of **5** in the organogels of **4** (Fig. 6). The emission color can be further changed by switching alternatively between UV and visible light irradiation when a photochromic dye such as spiropyran is doped to the organogel.

## 2.2 Gelators containing silole luminogens

Siloles are well-known luminogens with AIE characteristics. Many silole derivatives undergo self-assembly under certain
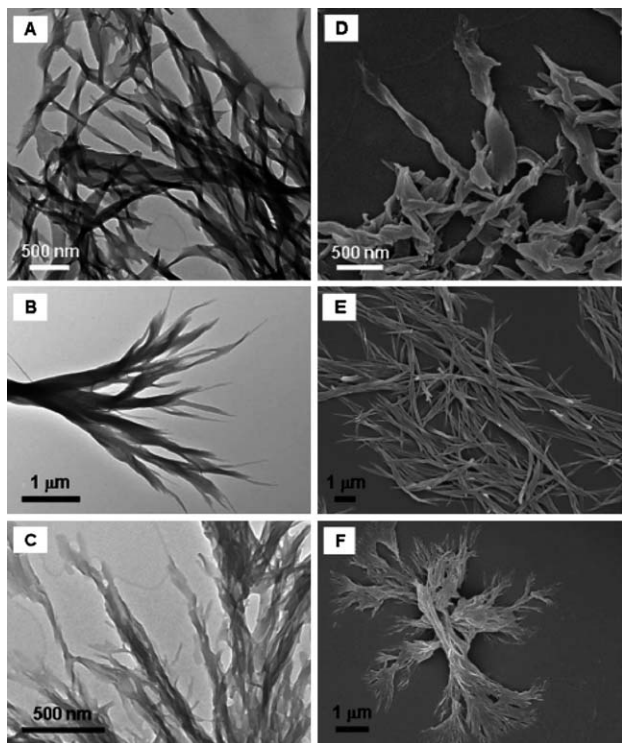

Fig. 3 (A–C) TEM and (D–F) SEM images for (A and D) gels of **3** formed in THF and precipitates of (B and E) **2** and (C and F) **3** obtained by cooling their hot, concentrated THF solutions. Reproduced with permission from ref. 73. Copyright (2012) The Royal Society of Chemistry.
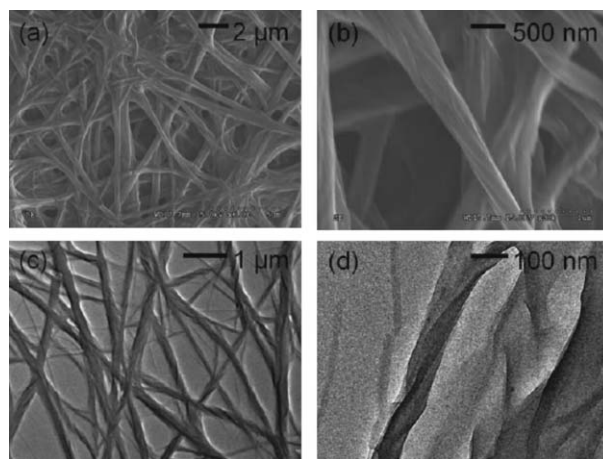
Fig. 4 (a and b) SEM and (c and d) TEM images of the xerogel of **4** formed in toluene with a concentration of 20 mg mL^{-1}. Reproduced with permission from ref. 74. Copyright (2010) Wiley-VCH.
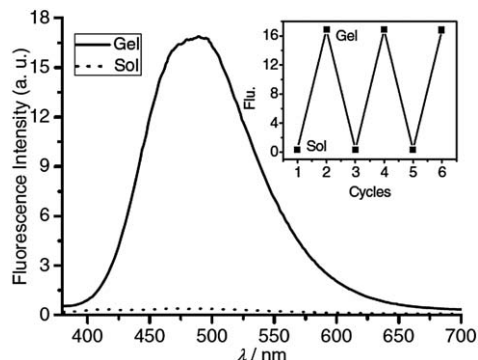
Fig. 5 Fluorescence spectra of solution of **4** and its organogels formed in toluene (20 mg mL^{-1}). Excitation wavelength: 365 nm. The inset shows the reversible fluorescence tuning by repeated heating and cooling cycles. Reproduced with permission from ref. 74. Copyright (2010) Wiley-VCH.
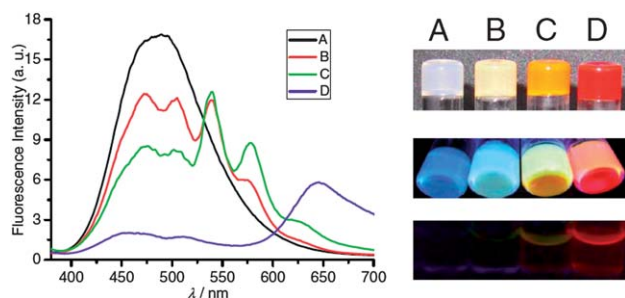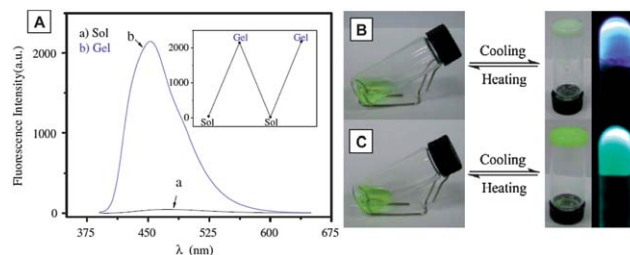

Fig. 6 (Left) Fluorescence spectra of organogels of **4** formed in toluene (20 mg mL^{-1}) (A) without and (B–D) with (B) 0.1 mM, (C) 1.0 mM and (D) 10 mM of **5**. Excitation wavelength: 365 nm. (Right) Photos of (top and middle) organogels and (bottom) the corresponding solutions taken under (top) daylight and (middle) UV light illumination. Reproduced with permission from ref. 74. Copyright (2010) Wiley-VCH.

conditions to form crystalline nanostructured materials such as nanofibers.[75–77] Incorporation of "soft" substituents that can induce strong intermolecular interactions into siloles is thus anticipated to generate AIE-active gelators. Zhang and co-workers[78] reported two silole-based gelators **6** and **7**, in which the urea and cholesterol moieties were attached to the 1-position of the 1-methyl-2,3,4,5-tetraphenylsilole core, respectively, through an amide functionality (Chart 4). The two luminogens exhibit similar AIE characteristics, as revealed by the large increase in the emission intensity upon aggregate formation in aqueous solution (Fig. 7A). Driven by the strong intermolecular interactions between the urea or cholesterol
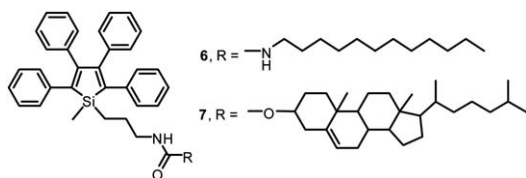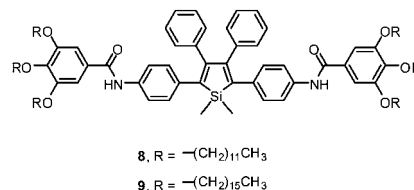

Fig. 7 (A) Fluorescence spectra of luminogen **6** in *n*-hexane (23 mg mL^{-1}) before and after gel formation. The inset shows the reversible emission switching at 453 nm by repeated sol–gel phase transition. Illustration of gel formation in (B) **6** (23 mg mL^{-1} in hexane) and (C) **7** (150 mg mL^{-1} in *n*-heptane), and the fluorescence photos of their gels taken under 365 nm UV illumination. Reproduced with permission from ref. 78. Copyright (2009) Elsevier.

groups, both **6** and **7** can form emissive organogels in non-polar solvents such as hexane, cyclohexane and heptane. The xerogels of **6** and **7** show worm-like structures (Fig. 8) and emit intensely due to the restriction of the IMR process of the silole unit. In addition, the PL process of both organogels is thermally responsive. Reversible transition between the sol and gel states can be achieved by alternative heating and cooling processes, which turns the emission of the organogels from dark to bright states and *vice versa* (Fig. 7B and C). This demonstrates a thermally driven fluorescence switch constructed from silole-containing organogels.

Wan and co-workers[79] prepared two 2,3,4,5-tetraphenylsiloles (**8** and **9**) with long alkoxyl chains at the 2,5-positions (Chart 5). Both luminogens form stable organogels in hydrocarbon solvents such as hexane, cyclohexane and *n*-decane by slow cooling of their hot solutions to room temperature. The gelation process was thermally reversible and the gels dissolved at elevated temperature. Like most silole derivatives, gelators **8** and **9** are almost non-
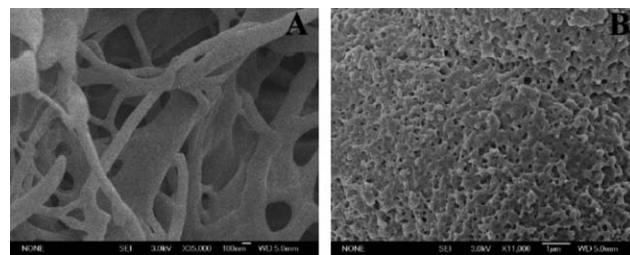
Fig. 8 SEM images of xerogels of (A) **6** in hexane and (B) **7** in *n*-heptane. Reproduced with permission from ref. 78. Copyright (2009) Elsevier.

Chart 4 Molecular structures of gelators fabricated from urea or cholesterol-containing silole derivatives.

Chart 5 Molecular structures of silole-based gelators containing alkoxyl chains with different lengths.

emissive in the solution state but their organogels fluoresce strongly at 519 nm upon photoexcitation with the intensity being ~100-fold higher than that in solution (Fig. 9).

Observation from polarized optical microscopy (POM) and field emission scanning electron microscopy (FE-SEM) shows that the xerogels of **8** and **9** possess 3D frameworks built from intertwisted and interlocked nanofibers (Fig. 10). The alkoxy chain has a strong impact on the self-assembly behaviors of the gelators as the morphology of their gels changes upon varying the chain length. Results from FT-IR and absorption analyses suggest that hydrogen bonding and π-stacking interactions are the main driving forces for organogel formation. These multiple weak interactions also work collectively to restrict the IMR process of phenyl rings attached at the silole core in the gel state and hence endow the organogels with efficient light emissions. Besides nanofibers, both **8** and **9** can self-organize into other nanomaterials such as molecular monolayers and liquid crystals.
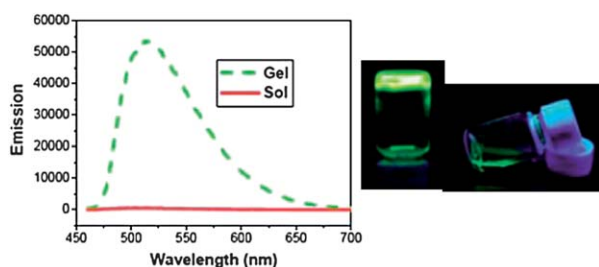
2.3 Gelators comprised of cyanostilbene units

In addition to propeller-like silole and TPE derivatives, cyano-substituted stilbenes were another class of widely studied AIE-

Fig. 9 (Left) Fluorescence spectra of solution and gels of **8** in dichloromethane (14 mg mL^{-1}). (Right) Fluorescent images of gels and solution of **8** taken under 365 nm UV irradiation. Reproduced with permission from ref. 79. Copyright (2010) The Royal Society of Chemistry.

Fig. 10 (a and b) POM and (c and d) FE-SEM images of xerogels of (a and c) **8** and (b and d) **9** formed in hexane (14 mg mL^{-1}). Reproduced with permission from ref. 79. Copyright (2010) The Royal Society of Chemistry.

active luminogens, which were first reported by Park and co-workers in 2002.[80] The AIE behaviors of these molecules are attributed to the formation of more coplanar conformations and J-aggregates in the condensed phase. These AIE-active luminogens possess good self-assembly properties and many fluorescent 1D nanowires with tunable emission colors have been fabricated through suitable molecular designs.[48,81]

Recently, Park and co-workers[82] synthesized a series of organogelators from cyanostilbene building blocks. A wholly π-conjugated aromatic gelator (**10**), named β-cyano-substituted distyrylbenzene, can undergo gelation readily in 1,2-dichloro-ethane (DCE) or dichloromethane by a heating and cooling method. The critical gelation concentration is as low as 0.8 wt% and the gelation process is thermoreversible. Observation from SEM shows that the xerogel of **10** possesses a 3D network formed by the entanglement of 1D fibrous nanoaggregates (Fig. 11). Due to the absence of a flexible alkyl chain, the molecules of **10** are stacked in a compact and ordered fashion, and its self-assembled 1D nanofibers are crystalline in nature and show good semiconductivity. The gels of **10** are highly emissive, emitting intense green light with a Φ_F value (52%) much higher than that in solution (1.6%). It is considered that the cooperative interplay of π–π stacking between phenyl rings and the dipole–dipole interaction between cyano groups drive the self-assembly process and contribute for the emission enhancement.
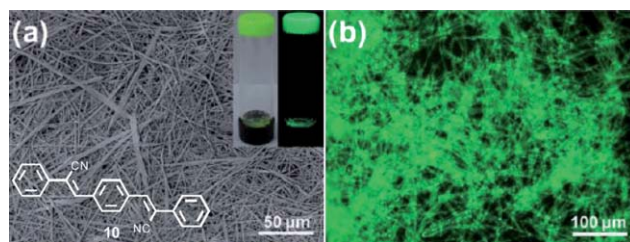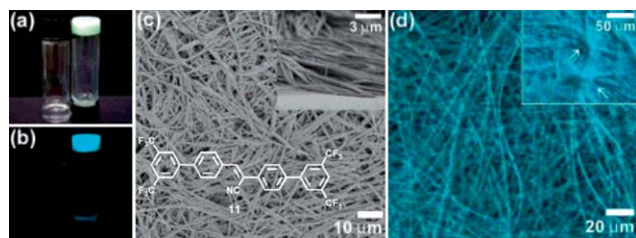
Park and co-workers[83] also found that the trifluoromethyl group functions similarly to an alkyl chain or steroidal unit in the gelation process. For example, a trifluoromethyl-substituted cyanostilbene derivative **11** shows good gelation ability in many organic solvents, such as DCE, toluene, chloroform and *tert*-butyl alcohol. Organogels of **11** are readily formed by a simple thermal treatment and the gelation process is completely thermoreversible. The SEM image of the gels reveals an entangled 3D network consisting of bundles of fibrous aggregates (Fig. 12). Whereas **11** is almost non-fluorescent in the solution state, it emits more intensely at the longer wavelength region in the gel state, thanks to the AIE-active cyanostilbene framework. Besides π-stacking interactions between aromatic rings, it is presumed that the tri-fluoromethyl groups can reinforce the intermolecular interactions and serve as essential alternative forces to promote the gelation process. Indeed, the control compounds with methyl groups instead of trifluoromethyl substituents
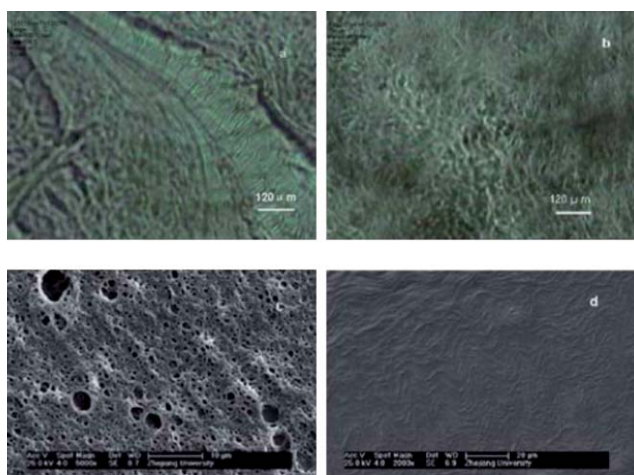
Fig. 11 (a) SEM and (b) fluorescence microscopic images of dried gels of **10** obtained from DCE. Reproduced with permission from ref. 82. Copyright (2011) The Royal Society of Chemistry.
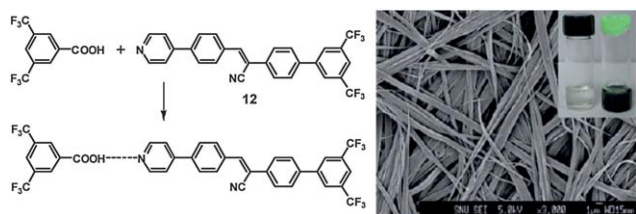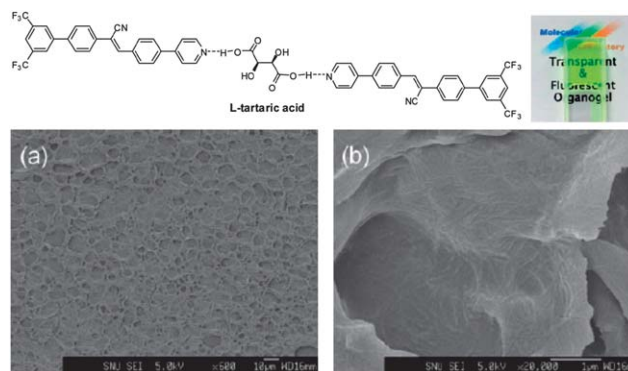
Fig. 12 (a and b) Photos of DCE solution of **11** (0.8 wt/vol%) at 60 °C (left vial) and the corresponding organogel at 20 °C (right vial) taken under (a) normal room illumination and (b) 365 nm UV irradiation. (c) SEM image of a dried gel of **11** formed in DCE. (d) Fluorescence microscopy image of organogel of **11**. The arrows shown in the inset indicate node where fibers of **11** are largely bundled and knotted. Reproduced with permission from ref. 83. Copyright (2004) American Chemical Society.

possess no gelation ability. Thus, the trifluoromethyl group may be a new choice in the gelator design rather than the widely used substituents such as alkyl chains, steroidal units, or amide functionalities, which are electronically saturated and hence may undermine the optoelectronic properties of the self-assembled nanomaterials. By doping a photochromic chromophore into the supramolecular organogels, a binary logic gate was constructed, in which light serves as the output in response to the dual inputs of UV irradiation and thermal heating.[84]

Replacement of one 3,5-bis(trifluoromethyl)phenyl group in **11** by a pyridine ring generates a new AIE-active gelator (**12**).[85] Although the luminogen exhibits no self-assembly property, it forms organogels in the presence of 3,5-trifluoromethyl benzoic acid (Fig. 13) or L-tartaric acid (Fig. 14). The pyridine ring in **12** enables formation of a hydrogen bond with 3,5-trifluoromethylbenzoic acid or L-tartaric acid. The resulting hydrogen-bonded complexes can undergo supramolecular self-assembly in DCE and immobilize organic solvents efficiently, affording translucent and highly emissive organogels with entangled and fibrillar aggregates. The emission of the gels is observed at the longer wavelengths than that in solution, suggesting that the complexes adopt a more planar conformation and pile up tightly in a J-aggregation fashion. Thanks to the chiral L-tartaric acid, the gels based on the complex of **12** and L-tartaric acid exhibit a strong circular dichroism signal.
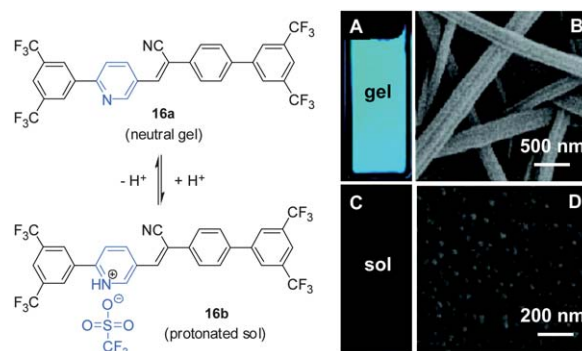

Fig. 14 (Upper layer) H-bonded complex formed from **12** and L-tartaric acid and the photograph of its gel obtained from **12** (1 wt%, 1 equiv.) and L-tartaric acid (0.5 equiv.) in DCE–THF mixture (10 : 1 v/v). (Bottom layer) (a and b) SEM images of dried gels of the H-bonded complex (1 wt%). Reproduced with permission from ref. 85. Copyright (2008) The Royal Society of Chemistry.
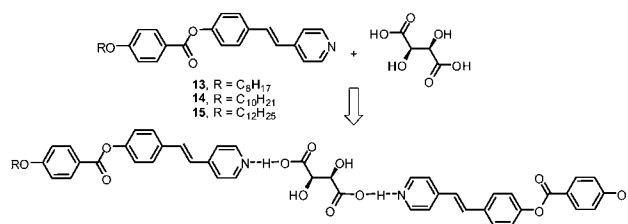
Chart 6 Molecular structures of gelators **13–15** and their complexes with L-tartaric acid.

With the aid of L-tartaric acid, binary organogels based on the gelators **13–15** were prepared by Zhao and coworkers.[86] Luminogens **13–15** also exhibit enhanced emission in the gel state due to the formation of multiple hydrogen bonds and J-aggregates (Chart 6).

"Smart" or "intelligent" materials change their properties in response to external stimuli or perturbations. Research on intelligent materials which are capable of reversibly switching their photophysical properties between two different states has great technological implications but is still in its infancy. By

Fig. 13 (Left) Schematic representation of the hydrogen (H)-bonded complex formed by **12** and 3,5-bistrifluoromethyl benzoic acid (BA). (Right) SEM image of partially dried gels of the H-bonded complex formed by **12** (1 wt%, 1 equiv.) and BA (1 equiv.) in DCE. The inset shows the photos of solution of **12** in DCE and gels of the H-bonded complex taken under daylight illumination. Reproduced with permission from ref. 85. Copyright (2008) The Royal Society of Chemistry.

Fig. 15 (A and C) Photographs of reversible sol–gel transition of **16** taken under illumination of a UV lamp. (B and D) SEM images of the neutral gel and protonated sol, respectively. Reproduced with permission from ref. 87. Copyright (2008) American Chemical Society.

combining the properties of luminogens **11** and **12**, Park and co-workers have designed stimuli-responsive fluorophors **16**, whose gels can reversibly and repeatedly modulate their morphology and/or physical properties by external stimuli such as temperature or pH changes.[87] Gelator **16a** is practically non-luminescent in the solution state but highly fluorescent upon gelation (Fig. 15A). As observed from the SEM image, the xerogel of **16a** consists of many long and entangled nanofibers that stabilize the gel state (Fig. 15B). Thermal- or photo-induced protonation of **16a** on the pyridine ring yields **16b**, which disassembles the fibrous aggregates of the gel with a concomitant decrease in the fluorescence intensity (Fig. 15C and D). The gel-to-sol phase transition is reversible and the light emission can be recovered by deprotonation of **16b**.

3 Organogels with conventional chromophores

3.1 Gelators from π-conjugated planar 1,3,4-oxadiazole derivatives

1,3,4-Oxadiazole is widely used as a building block for the construction of electron-transporting materials due to its electron-deficient nature. Numerous 1,3,4-oxadiazole-based materials have been prepared, which exhibit promising applications as active materials in optoelectronic devices. However, ordered nanomaterials from 1,3,4-oxadiazole derivatives are rarely reported. Recently, Li and co-workers[88] devoted much effort to study the self-assembly behaviors of bis(1,3,4-oxadiazole)s and made noteworthy contributions to this area of research. For example, a twin-tapered bi(1,3,4-oxadiazole) named 2,2′-bis(3,4,5-trioctanoxyphenyl)bis(1,3,4-oxadiazole) (**17**) was found to exhibit solvent polarity-dependent fluorescence due to the presence of an electron donor–acceptor pair in the molecular structure (Chart 7). **17** possesses good self-assembly property and forms helical nanofibers as well as immobile organogel by
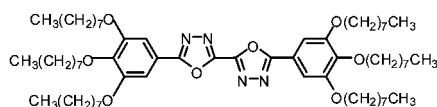
cooling its hot ethanol solution to room temperature. The xerogel of **17** exhibits a 3D network with flat ribbons, as revealed by the FE-SEM image (Fig. 16). Although **17** fluoresces weakly at 495 nm in ethanol solution with a Φ_F value of 2%, its gel and xerogel show stronger and bluer emission at 424 nm and 408 nm, respectively. The Φ_F value of the xerogel is determined to be 40%. The enhanced fluorescence at the shorter wavelength upon gel formation should be due to the tight π-stacking and the formation of J-aggregates (Fig. 17), where the core part comprised of two 1,3,4-oxadiazole and phenyl rings of one molecule becomes more coplanar and stacks tightly with that of its neighbor. This relieves the interaction of the gelator with solvent molecules and thus reduces the solvent effect on the PL process. The electron-donating property of 3,4,5-trioctanoxy-phenyl and electron-accepting character of 1,3,4-oxadiazole can induce intermolecular electron communication, thus promoting such slipped J-type stacking.

Further studies disclosed that this achiral gelator **17** can undergo hierarchical self-assembly from a lyotropic liquid crystal to a helical fibrous organogel by cooling its DMF solution with a concentration above 0.6 wt% (Fig. 18 and 19).[89] The formation of such a supramolecular structure is dependent on the solvent and concentration. It is considered that the intermolecular π–π interactions between aromatic segments are the main driving forces for the formation of fibrous nanomaterials, while the weak van der Waals forces between alkyl chains are the cause of the helical fine structures of the fibers made of achiral **17**. The nature of the solvent also plays a key role in the gelation process.

Fig. 17 Packing mode of the xerogel of **17**. Reproduced with permission from ref. 88. Copyright (2009) American Chemical Society.

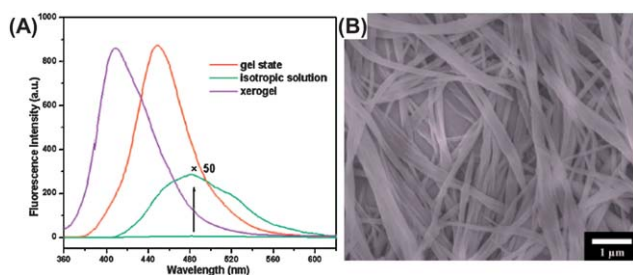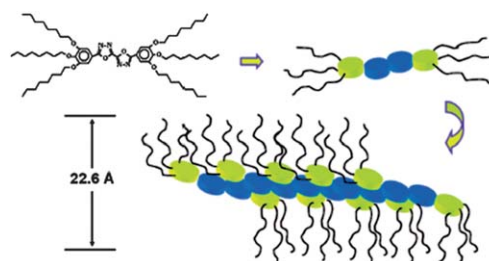**Chart 7** Chemical structure of gelator **17**.

Fig. 16 (A) Fluorescence spectra of isotropic solution, gel and xerogel of **17** in ethanol (0.7 wt%). (B) FE-SEM image of the xerogel of **17** obtained from gel in ethanol (0.7 wt%). Reproduced with permission from ref. 88. Copyright (2009) American Chemical Society.
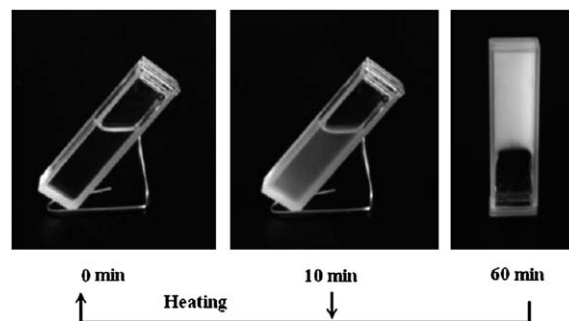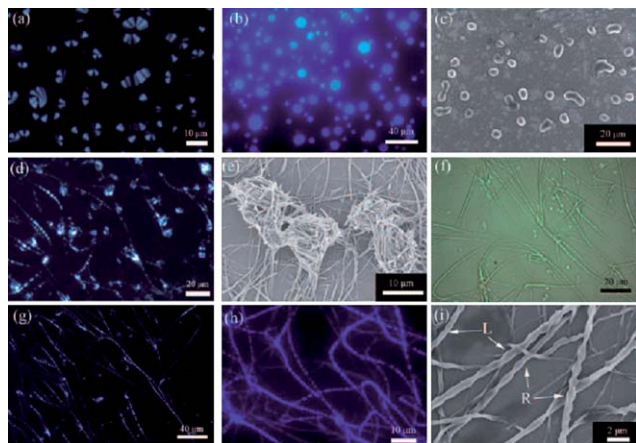

Fig. 18 Photographs show the progressive formation of a lyotropic liquid crystal and organogel from **17** in DMF at 1.0 wt% upon heating its organogel to obtain an isotropic solution and then holding at room temperature for different time periods. Reproduced with permission from ref. 89. Copyright (2011) Wiley-VCH.

Fig. 19 (a, d and g) POM, (b and h) PLM and (c) SEM and (f) optical images of **17** obtained by cooling its isotropic solution in DMF at 1.0 wt% and holding at room temperature for (a–c) 10, (c and e) 20 and (f–h) 30 min. (i) SEM image of the xerogel of **17** from gel in DMF (1.0 wt%). Reproduced with permission from ref. 89. Copyright (2011) Wiley-VCH.

3.2 Dendritic gelators

Hydrogen bonding is a stronger intermolecular force than π-stacking interactions and van der Waals forces for gel formation. It is also an important driving force in the process of supramolecular self-assembly in nature. Park and co-workers[90] reported a dendritic gelator based on a hydrogen bonding motif. A 1,3,4-oxadiazole-based benzene-1,3,5-tricarboxamide gelator **18** shows a robust gelation property in THF, 1,4-dioxane and most chlorinated solvents. Immobile organogels can be readily obtained by cooling its hot dilute chloroform solution (0.05 wt%) to room temperature (Fig. 20). The organogels can be converted to a clear solution upon addition of a small amount of methanol due to the disruption of the formation of an intermolecular hydrogen bond. It is presumed that the molecules align in a face-to-face fashion via axial hydrogen bond formation between the amide groups to form 1D nanofibers. The xerogels of **18** exhibit a morphology composed of intertwined boundless fibrils and large ropes formed from intertwisted fibrils (Fig. 21).

Whereas **18** is almost non-fluorescent in solution, its gels are highly emissive. The PL intensity of the gels formed in
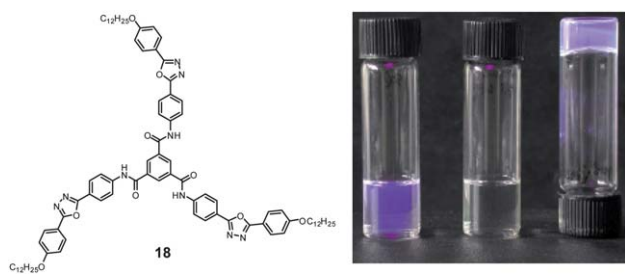
Fig. 20 Chemical structure of **18** and its fluorescent images in (left) CHCl₃ (20 mM), (middle) 0.1 wt% solution in CHCl₃–methanol (9 : 1 v/v) and (right) 0.1 wt% gel in CHCl₃ taken under 365 nm illumination. Reproduced with permission from ref. 90. Copyright (2004) The Royal Society of Chemistry.
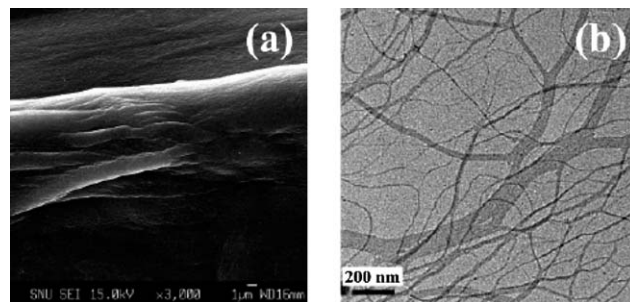

Fig. 21 (a) SEM and (b) TEM images of the xerogel of **18** formed in chloroform solution (0.1 wt%). Reproduced with permission from ref. 90. Copyright (2004) The Royal Society of Chemistry.

chloroform is 100-fold higher than that in the solution state. A similar emission enhancement was also observed for the hydrogen-bonded aggregates. A time-resolved fluorescence study reveals that the hydrogen bonded aggregates have a longer lifetime than the monomer, suggesting that a non-radiative relaxation process such as intersystem crossing or twisted intramolecular charge transfer (TICT) is suppressed in the gel state and hence makes the organogels highly emissive.

Barluenga and co-workers[91] reported a dendritic gelator **19** composed of a 1,6-bis(4-hydroxyphenyl)-3-hexen-1,5-diyne core and 3,4,5-tris(3,4,5-trihydroxybenzyloxy)benzoic acid-based dendrons (Chart 8). This dendritic gelator undergoes columnar self-organization to yield not only liquid crystals but also organogels. It can supramolecularly self-assemble to form organogels in cyclohexane and dodecane at low temperature. Observation via SEM reveals that the xerogel of **19** exhibits a 3D-network with nano-scaled fibers (Fig. 22). The porous structure enables the gel to retain solvent molecules efficiently. Experimental and calculation results show that the interactions between the gelator and different solvent molecules have great impact on the aggregation manner and the gelation process.

Interestingly, **19** shows weak fluorescence in solution but gives rise to strong fluorescence in the gel state (Fig. 23), although its chromophoric core shows an opposite fluorescence behavior. The sol–gel transition and hence the PL change are reversible and can be achieved by precise control on the temperature. The fact that the core of **19** is emissive in solution but non-emissive in the aggregated state is due to the formation of detrimental species such as excimer. After encapsulated by
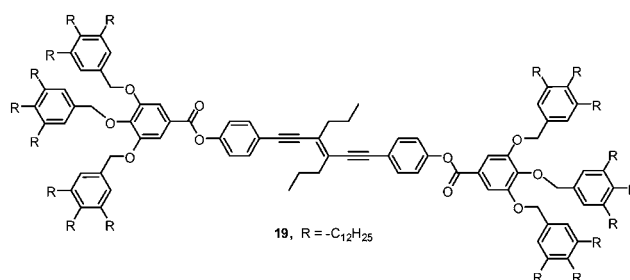
Chart 8 Chemical structure of gelator **19**.
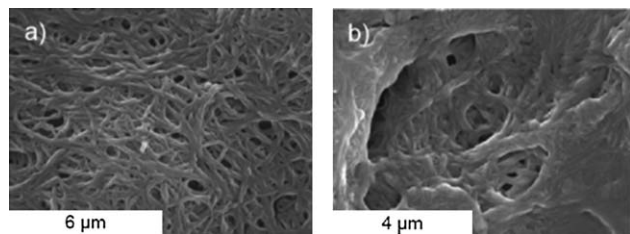
Fig. 22 SEM images of xerogels of **19** formed in (a) dodecane (×10 000) and (b) cyclohexane (×14 000). Reproduced with permission from ref. 91. Copyright (2011) American Chemical Society.
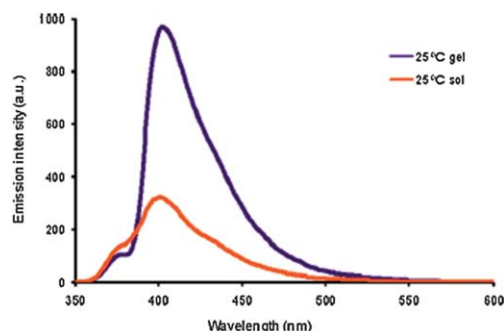
Fig. 23 Emission spectra of **19** in cyclohexane at a concentration of 3 wt% at room temperature in the sol and gel states, excited at 335 nm. Reproduced with permission from ref. 91. Copyright (2011) American Chemical Society.

bulky dendrons, the emission of the core becomes weaker owing to the non-radiative energy relaxation caused by intramolecular vibration. On the other hand, in the gel state, the close packing between molecules of **19** becomes difficult due to the presence of the dendritic unit as well as solvent molecules. At the same time, the molecular structure becomes stiffer and the intramolecular motion is hampered due to physical constraints. Both factors can reduce the non-radiative energy decay, resulting in the enhanced emission as the organogels form.

3.3 Carbazole-based gelators

Carbazole is a well-known π-conjugated chromophore with good electron-donating ability. Its derivatives have been widely used as light-emitting and hole-transporting materials, photovoltaic materials, nonlinear materials, etc. Many tailored carbazole derivatives show good supramolecular self-assembly capabilities. For instance, Moore and co-workers[42] developed a series of large macrocyclic aromatic molecules based on carbazole. These macro rings are prone to 1D self-assembly through a strong π–π interaction as well as van der Waals forces to afford nanofibers. Tian and co-workers studied the self-assembly of carbazole and anthracene-based luminogens and found that they were capable of forming unique nanorings with enhanced fluorescence.[61] However, organogelators based on carbazole are rarely reported.

Recently, Lu and co-workers[92] prepared a series of carbazole-based organogelators with *tert*-butyl substituents instead

of long alkyl chains or steroidal groups (Chart 9). Compound **20** can facily form organogels in apolar solvents including cyclohexane, hexane and petroleum ether by cooling its hot solutions to room temperature with a concentration of 0.2 wt %. Incorporation of an additional carbazole ring into the molecular structure of **20** has weakened the gelation ability of the resulting molecule (**21**). However, the control molecules without *tert*-butyl substituents do not show any gelation ability at all. In addition, the generation of the rigid dendritic gelators also exerts a significant impact on the gelation process. For example, compound **23** can form two-component organogels with 1,6-diaminohexane by cooling its hot toluene solution to room temperature. No organogels, however, are formed from **24** under the same conditions.[93] In contrast, **24** can form gels by ultrasound irradiation of its chloroform–hexane or chloroform–cyclohexane mixture, which is not found in **23**. No gelation ability was observed from a third-generated dendrimer. Lu and co-workers further created a flexible dendritic gelator **22** based on *tert*-butyl substituted carbazoles.[94] An amide group is chosen as the linker because it is an excellent hydrogen bonding site to impart good self-assembly ability. Organogels of **22** are facily formed in dimethylsulfoxide (DMSO) and its mixtures, showing a high gel–sol transition temperature of 70 °C and a low critical gelation concentration of 6.2×10^{-4} M.
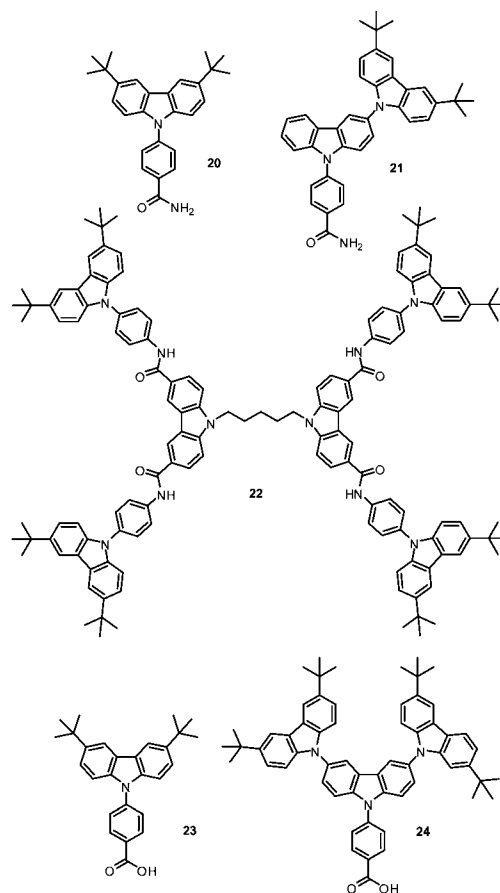

Chart 9 Molecular structures of carbazole-based dendritic gelators.

All the xerogels of *tert*-butyl-substituted carbazole-based gelators exhibit 3D networks with entangled bundles of nano-fibres (Fig. 24). Hydrogen bonding coupled with π-stacking interactions between the carbazole units are the main driving forces for the gel formation. The formation of hydrogen bonds between the amide or carboxylic acid groups may promote the formation of dimers and thus give rise to a lamellar organiza-tion. All the organogels exhibit higher fluorescence intensity than their isolated molecules in solutions, presenting a phenomenon of gelation-enhanced emission (Fig. 25). This is the exact opposite of most carbazole-based materials, whose strong emission in solutions is quenched at the aggregated

state. It is deemed that the formation of J-aggregates and the restriction of the IMR process in the gel state are the possible reasons for the emission enhancement. Such an organogel shows potential application as a fluorescent chemosensor for fluoride anion detection.

# 4 Organogels with excited-state intramolecular proton transfer features

2-(2′-Hydroxyphenyl)benzoxazole (HPB) is a remarkable chro-mophore and has been extensively studied because of its interesting and reversible excited-state intramolecular proton transfer (ESIPT) feature, which endows it with tunable emission intensity and color. Recently, Lee and co-workers[95] developed two organogelators **25** and **26** based on HPB (Chart 10). Gelator **25** can form stable organogels by adding cold toluene to its hot DMF solution (0.5%, DMF–toluene 1 : 9 v/v). It self-assembles into fibrous nanoaggregates, where their entanglement forms gel with the 3D network (Fig. 26). Whereas the gelators are weakly fluorescent in DMF solution ($\Phi_F = 1.4\%$), their organo-gels are highly emissive with a Φ_F value of 34.7%. In the process of gelation, the HPB units of the molecules of **25** are aggregated. This inhibits the free rotation of the benzoxazole ring and promotes the ESIPT process from the hydroxyl proton to the nitrogen atom, thus converting the molecule from an enol tautomer to a keto form (Chart 11). Due to its more planar structure, the keto tautomer shows a stronger π-stacking interaction and hence a higher tendency for gel formation with the assistance of hydrogen bond formation between the urea moieties and the van der Waals forces between the octyl chains. Moreover, as the keto tautomer is more fluorescent than its enol cousin, its organogels thus exhibit strong emission
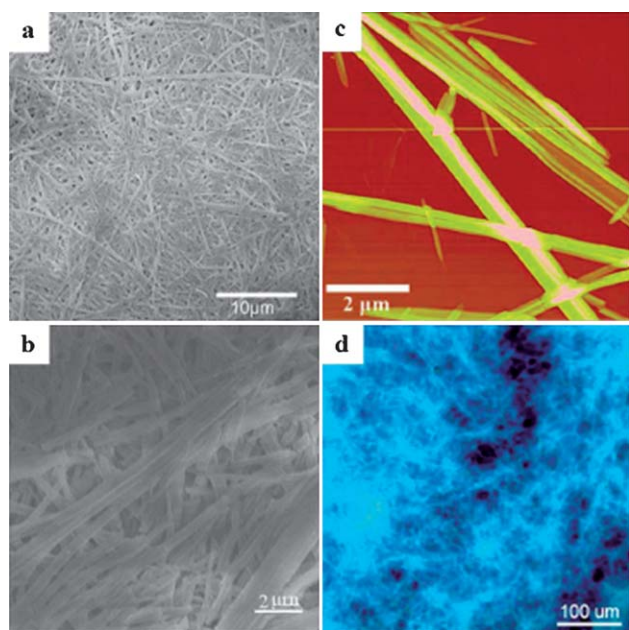

Fig. 24 (A and B) SEM, (C) AFM and (D) fluorescence microscopic images of the xerogel of **22** obtained from DMSO. Excitation wavelength: 330–385 nm. Reproduced with permission from ref. 94. Copyright (2011) The Royal Society of Chemistry.
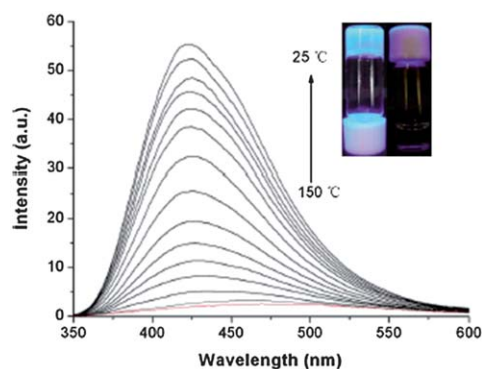
Fig. 25 Temperature-dependent fluorescence spectra of **22** in DMSO (black) (8.3×10^{-4} M, excitation wavelength: 299 nm) and in THF (red, 8.3×10^{-4} M, 25 °C). Inset: photograph of gel and solution of **22** in DMSO taken under 365 UV irradiation. Reproduced with permission from ref. 94. Copyright (2011) The Royal Society of Chemistry.
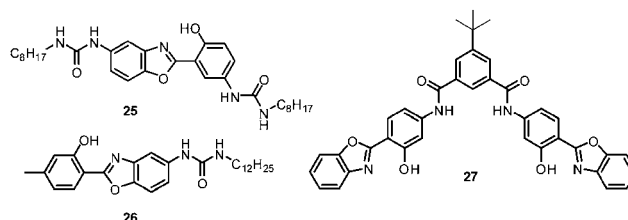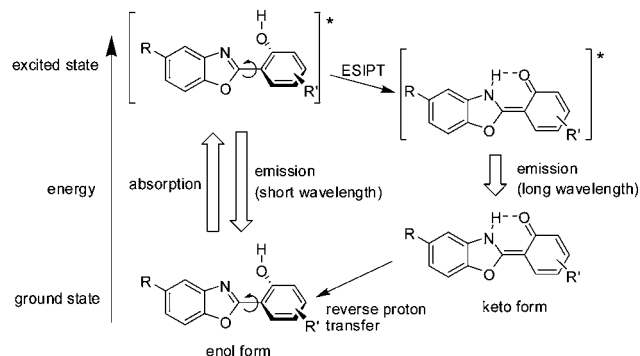

Chart 10 Molecular structures of organogelators consisting of 2-(2′-hydroxy-phenyl)benzoxazole units.
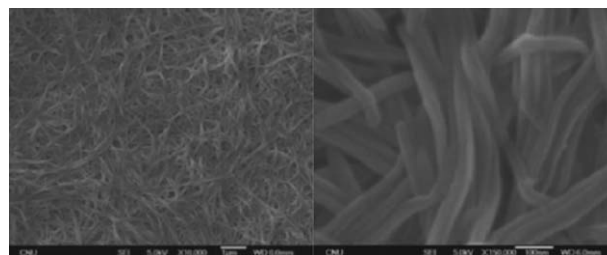
Fig. 26 FE-SEM images of the xerogel of **25**. Scale bar (mm): 1 (left) and 100 (right). Reproduced with permission from ref. 95. Copyright (2008) The Royal Society of Chemistry.
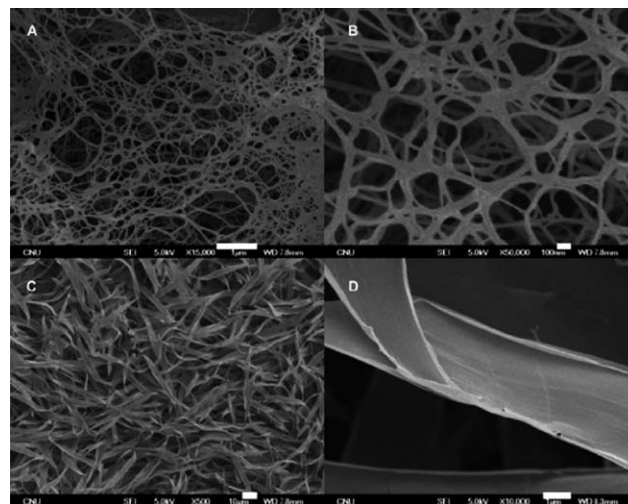
Chart 11 Proposed mechanism for ESIPT of HPB. Reproduced with permission from ref. 95. Copyright (2008) The Royal Society of Chemistry.

Fig. 28 FE-SEM images of freeze-dried gels of **26** obtained from (A and B) CCl_4 and (C and D) cyclohexane. Concentration: 1% w/v; scale bar (mm): (A) 26, (B) 100, (C) 10 and (D) 1. Reproduced with permission from ref. 96. Copyright (2010) Elsevier.

enhancement. Addition of a fluoride anion into the mixture disrupts the formation of hydrogen bonds and leads to gel-to-sol transition and emission change, demonstrating the potential application of the organogel as a fluorescent sensor for fluoride anion detection.

Similar gelation-enhanced emission was also observed in gelator **26**.[96] This gelator also exhibits ESIPT characteristic due to the presence of a HPB core. It possesses thermally reversible gelation ability in various solvents (Fig. 27A) and the morphology of the resulting gels depends strongly on the choice of solvent. For example, **26** forms gel with a fibrillar structure in carbon tetrachloride but a ribbon-like one in cyclohexane (Fig. 28). This should be related to the different affinities of the gelator with the solvent molecule. Similar to those of **25**, the gels of **26** obtained from both solutions exhibit dramatically enhanced fluorescence with respect to their solutions. The predominant formation of a planar keto

tautomer enables the gel to fluoresce strongly at a longer wavelength and facilitates π-stacking for gel formation. The gel disintegrates in the presence of diethylchlorophosphate (DCP) liquid owing to the breakage of the intra- and inter-molecular hydrogen bonds. On the other hand, a notable color change was observed when the gel was exposed to DCP vapor (Fig. 27B and C), suggesting that it is a sensitive chemosensor for nerve gas detection.

Yang and co-workers[97] prepared a HPB-based gelator **27** without alkyl chains (Chart 10) and found that it can form uniform, stable and thermoreversible organogels in the THF–cyclohexane mixture (Fig. 29). The xerogel of **27** possesses a 3D network consisting of tangled nanoribbons with a uniform width of ∼100 nm and a length of over several tens of micrometers (Fig. 30). It is considered that the formation of hydrogen bonds between J-aggregated dimers of **27** through N⋯π and O⋯π stacking interactions of the oxazole rings have driven the self-assembly of the molecules efficiently. Similar to other HPB-based ESIPT gelators, **27** is weakly fluorescent in the solution state but emits intense sky blue light in the gel state. The ESIPT phenomenon, J-aggregate formation and restriction of the TICT process are speculated to be responsible for the efficient emission in the gel state.
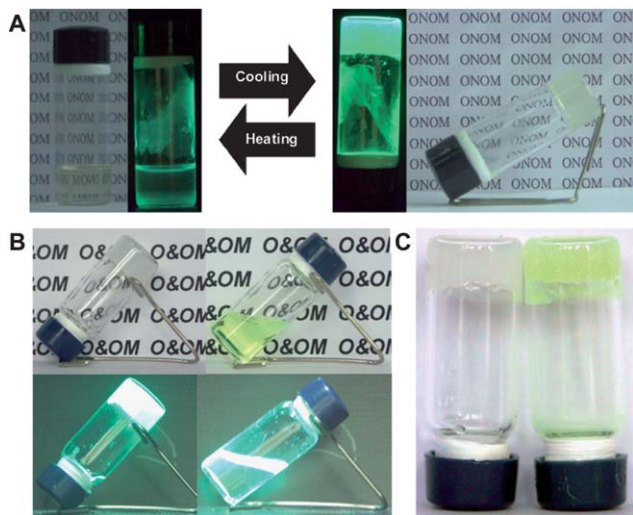
Fig. 27 (A) Photographs demonstrate the sol–gel process of **26** in CCl_4 (1% w/v) aided by heating and cooling processes. Photographs of gels of **26** obtained from CCl_4 (1% w/v) (B) before (left) and after (right) addition of DCP liquid (100 equiv.) taken under ambient (top) and UV (bottom) light. (C) Photos of gels of **26** in CCl_4 before (left) and after (right) exposure to DCP vapor. Reproduced with permission from ref. 96. Copyright (2010) Elsevier.
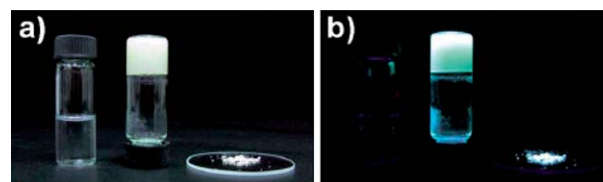

Fig. 29 Photographs of **27** in THF solution and gel (0.67 wt% in THF–cyclohexane mixture 2 : 3 v/v) state and solid powder states taken under (a) normal room illumination and (b) 365 nm UV irradiation. Reproduced with permission from ref. 97. Copyright (2012) The Royal Society of Chemistry.
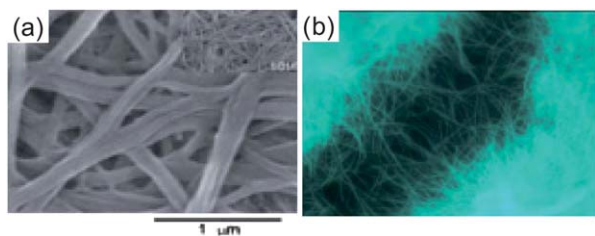
Fig. 30 (a) FE-SEM and (b) fluorescence microscopic images of xerogels of **27** (0.67 wt% in THF–cyclohexane mixture 2 : 3 v/v) at room temperature. Reproduced with permission from ref. 97. Copyright (2012) The Royal Society of Chemistry.

Nayak and co-workers[98,99] developed a series of photoactive gelators based on salicylanilide with ESIPT features (Chart 12). Gelators **28** and **29** can undergo self-assembly to form organogels in nonpolar solvents such as *n*-hexane and dodecane driven by π–π stacking interactions and both inter- and intramolecular hydrogen bonds. Analysis by FE-SEM reveals that **28** and **29** self-assemble into gels with lamellar and hexagonal columnar nanostructures, respectively (Fig. 31). Whereas these gelators are almost non-fluorescent in solutions, their organogels are strong emitters (Fig. 32).
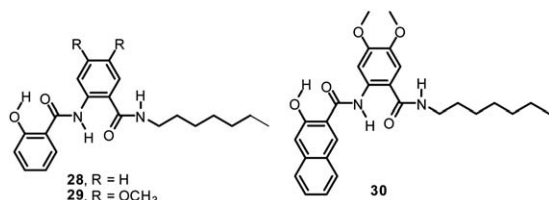

**Chart 12** Chemical structures of ESIPT-type gelators.
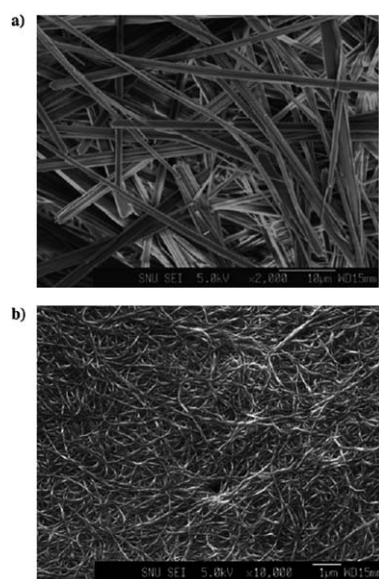
Fig. 31 FE-SEM images of xerogels of (a) **28** and (b) **29**. Reproduced with permission from ref. 98. Copyright (2010) Wiley-VCH.

Gelator **30** consisting of a hydroxyl naphthanilide functionality shows a similar TICT effect and gelation-enhanced emission as salicylanilide-based gelators. The formation of an intramolecular hydrogen bond can restrict both the intramolecular rotation and the TICT process, which promotes the radiative decay of excitons and imparts the gels of **30** with enhanced emission. The coplanarity of the molecule also becomes better, which is favorable for the formation of J-aggregates.

In addition to gelators with salicylanilide or hydroxyl naphthanilide groups show gelation-enhanced emission, those carrying salicylideneaniline units also show large emission enhancement in the gel state. Ihara and co-workers[100] prepared a TICT-active gelator **31** based on a salicylideneaniline derivative with cholesterol units (Fig. 33). This luminogen can self-assemble into left-handed 1D nanofibers, where their entanglement forms thicker fibers and subsequently a 3D network aided by π-stacking interactions between the aromatic rings and van der Waals forces between the cholesterol units. Upon gel formation, the fluorescence intensity is increased by more than 1000 times in comparison with that in the solution, which is attributed to the formation of J-aggregates and restriction of the IMR process. The organogels of **31** are photochromic and the sol–gel transition is reversibly driven by a thermal process. UV irradiation induces the isomerization of the salicylideneaniline units. This changes the packing of the molecules in the gel state and hence weakens the fluorescence of the gels.
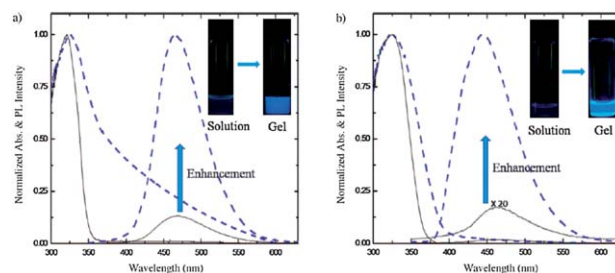
Fig. 32 Normalized UV/Vis absorption and PL spectra, and fluorescent photographs of (a) **28** and (b) **29** in the solution (solid line) and gel (dashed line) states. Reproduced with permission from ref. 98. Copyright (2010) Wiley-VCH.
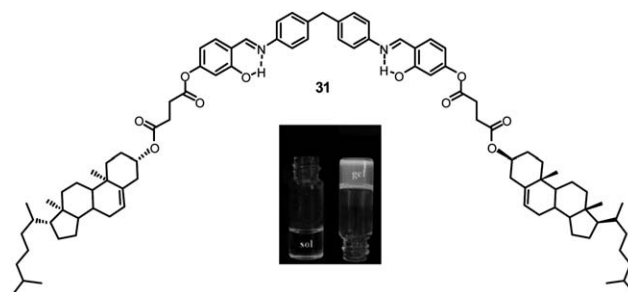
Fig. 33 Molecular structure of salicylideneaniline-based gelator **31** and photographs of its gels in a benzene–cyclohexane mixture and solution in benzene (0.1 wt/vol%) taken under 365 nm UV irradiation. Reproduced with permission from ref. 100. Copyright (2007) Wiley-VCH.

5 Conclusion

Fluorescent supramolecular organogels are intriguing soft materials with significant academic value and diverse applications. They are deemed to be "smart" materials for their sensitive response to multiple external stimuli for sol–gel transition. Since structure determines property, better understanding of their structure–property relationship can guide the future rational design of gelators for supramolecular organogels by a molecular engineering endeavor. After the observation of the AIE phenomenon in 2001, luminogenic materials with AIE characteristics have attracted particular research interest due to their potential applications in optics, electronics and environmental and biological sciences. In this review, an AIE motif is introduced into the self-assembled organogel systems. The remarkable progress in the investigation and development of fluorescent self-assembled organogels based on low molecular weight luminogenic materials with gelation-enhanced emission characteristics is described. Rationally designed gelators with typical AIE luminogens such as TPE, silole, cyanostilbene, and nonclassical AIE luminogens such as carbazole-based dendrimers, 1,3,4-oxadiazole derivatives and ESIPT dyes have shown excellent self-assembling ability to generate highly emissive organogels. The restriction of the IMR process and J-aggregate formation are main reasons for the enhanced emission of the gelators in the gel state. Further advancement in the research on fluorescent organogels will allow them to serve as promising alternatives for optoelectronics and fluorescent sensors.

Acknowledgements

References

1 G. John, S. R. Jadhav, V. M. Menon and V. T. John, *Angew. Chem., Int. Ed.*, 2012, **51**, 1760.

2 J. W. Steed, *Chem. Commun.*, 2011, **47**, 1379.

3 M. George and R. G. Weiss, *Acc. Chem. Res.*, 2006, **39**, 489.

4 A. Ajayaghosh and V. K. Praveen, *Acc. Chem. Res.*, 2007, **40**, 644.

5 A. Ajayaghosh, V. K. Praveen and C. Vijayakumar, *Chem. Soc. Rev.*, 2008, **37**, 109.

6 A. R. Hirst, B. Escuder, J. F. Miravet and D. K. Smith, *Angew. Chem., Int. Ed.*, 2008, **47**, 8002.

7 B. Song, H. Wei, Z. Q. Wang, X. Zhang, M. Smet and W. Dehaen, *Adv. Mater.*, 2007, **19**, 416.

8 C. Wang, D. Zhang and D. Zhu, *Langmuir*, 2007, **23**, 1478.

9 D. Das, T. Kar and P. K. Das, *Soft Matter*, 2012, **8**, 2348.

10 S. Banerjee, R. K. Das and U. Maitra, *J. Mater. Chem.*, 2009, **19**, 6649.

11 C. Wang, Z. Wang, D. Zhang and D. Zhu, *Chem. Phys. Lett.*, 2006, **428**, 130.

12 Y. Kamikawa and T. Kato, *Langmuir*, 2007, **23**, 274.

13 S. Das, S. Varghese and N. S. S. Kumar, *Langmuir*, 2010, **26**, 1598.

14 C. Wang, Q. Chen, F. Sun, D. Zhang, G. Zhang, Y. Huang, R. Zhao and D. Zhu, *J. Am. Chem. Soc.*, 2010, **132**, 3092.

15 A. R. Hirst, B. Escuder, J. F. Miravet and D. K. Smith, *Angew. Chem., Int. Ed.*, 2008, **47**, 8002.

16 N. M. Sangeetha and U. Maitra, *Chem. Soc. Rev.*, 2005, **34**, 821.

17 X. Chen, Z. Huang, S.-Y. Chen, K. Li, X.-Q. Yu and L. Pu, *J. Am. Chem. Soc.*, 2010, **132**, 7297.

18 M.-O. M. Piepenbrock, G. O. Lloyd, N. Clarke and J. W. Steed, *Chem. Rev.*, 2010, **110**, 1960.

19 F. Fages, *Angew. Chem., Int. Ed.*, 2006, **45**, 1680.

20 M. Shirakawa, N. Fujita and S. Shinkai, *J. Am. Chem. Soc.*, 2005, **127**, 4164.

21 J. H. Jung, Y. Ono, K. Hanabusa and S. Shinkai, *J. Am. Chem. Soc.*, 2000, **122**, 5008.

22 K. J. C. van Bommel, M. C. A. Stuart, B. L. Feringa and J. van Esch, *Org. Biomol. Chem.*, 2005, **3**, 2917.

23 H. Tang, X. Duan, X. Feng, L. Liu, S. Wang, Y. Li and D. Zhu, *Chem. Commun.*, 2009, 641.

24 K. Sugiyasu, N. Fujita and S. Shinkai, *Angew. Chem., Int. Ed.*, 2004, **43**, 1229.

25 C. Vijayakumar, V. K. Praveen and A. Ajayaghosh, *Adv. Mater.*, 2009, **21**, 2059.

26 A. Shome, S. Dutta, S. Maiti and P. K. Das, *Soft Matter*, 2011, **7**, 3011.

27 F. S. Kim, G. Ren and S. A. Jenekhe, *Chem. Mater.*, 2011, **23**, 682.

28 S. S. Babu, S. Prasanthkumar and A. Ajayaghosh, *Angew. Chem., Int. Ed.*, 2012, **51**, 1766.

29 A. Ajayaghosh, R. Varghese, V. K. Praveen and S. Mahesh, *Angew. Chem., Int. Ed.*, 2006, **45**, 3261.

30 V. K. Praveen, S. J. George, R. Varghese, C. Vijayakumar and A. Ajayaghosh, *J. Am. Chem. Soc.*, 2006, **128**, 7542.

31 A. Ajayaghosh, C. Vijayakumar, V. K. Praveen, S. S. Babu and R. Varghese, *J. Am. Chem. Soc.*, 2006, **128**, 7174.

32 A. Ajayaghosh, V. K. Praveen, C. Vijayakumar and S. J. George, *Angew. Chem., Int. Ed.*, 2007, **46**, 6260.

33 N. Mohmeyer, D. B. Kuang, P. Wang, H. W. Schmidt, S. M. Zakeeruddin and M. Gratzel, *J. Mater. Chem.*, 2006, **16**, 2978.

34 S. Diring, F. Camerel, B. Donnio, T. Dintzer, S. Toffanin, R. Capelli, M. Muccini and R. Ziessel, *J. Am. Chem. Soc.*, 2009, **131**, 18177.

35 J. H. Kim, Y. Jung, J. W. Chung, B. K. An and S. Y. Park, *Small*, 2009, **5**, 804.

36 C. Wang, Q. Chen, F. Sun, D. Zhang, G. Zhang, Y. Huang, R. Zhao and D. Zhu, *J. Am. Chem. Soc.*, 2010, **132**, 3092.

37 Y. Liu, X. Liu, Y. Wu, B. Sun, M. Zhu, M. Takafuji and H. Ihara, *Chem. Commun.*, 2010, **46**, 430.

38 T. Suzuki, S. Shinkai and K. Sada, *Adv. Mater.*, 2006, **18**, 1043.

39 H. Maeda, Y. Haketa and T. Nakanishi, *J. Am. Chem. Soc.*, 2007, **129**, 13661.

40 P. Mukhopadhyay, Y. Iwashita, M. Shirakawa, S. Kawano, N. Fujita and S. Shinkai, *Angew. Chem., Int. Ed.*, 2006, **45**, 1592.

41 H. Lee, S. H. Jung, W. S. Han, J. H. Moon, S. Kang, J. Y. Lee, J. H. Jung and S. Shinkai, *Chem.–Eur. J.*, 2011, **17**, 2823.

42 L. Zang, Y. Che and J. S. Moore, *Acc. Chem. Res.*, 2008, **41**, 1596.

43 H. Wu, L. Xue, Y. Shi, Y. Chen and X. Li, *Langmuir*, 2011, **27**, 3074.

44 H. Tsumatori, T. Nakashima and T. Kawai, *Org. Lett.*, 2010, **12**, 2362.

45 A. Kaeser and A. P. H. J. Schenning, *Adv. Mater.*, 2010, **22**, 2985.

46 F. Camerel, L. Bonardi, M. Schmutz and R. Ziessel, *J. Am. Chem. Soc.*, 2006, **128**, 4548.

47 S. S. Babu, K. K. Kartha and A. Ajayaghosh, *J. Phys. Chem. Lett.*, 2010, **1**, 3413.

48 B.-K. An, J. Gierschner and S. Y. Park, *Acc. Chem. Res.*, 2012, **45**, 544.

49 J. Luo, Z. Xie, J. W. Y. Lam, L. Cheng, H. Chen, C. Qiu, H. S. Kwok, X. Zhan, Y. Liu, D. Zhu and B. Z. Tang, *Chem. Commun.*, 2001, 1740.

50 Z. Zhao, P. Lu, J. W. Y. Lam, Z. Wang, C. Y. K. Chan, H. H. Y. Sung, I. D. Williams, Y. Ma and B. Z. Tang, *Chem. Sci.*, 2011, **2**, 672.

51 Y. Hong, J. W. Y. Lam and B. Z. Tang, *Chem. Commun.*, 2009, 4332.

52 Y. Hong, J. W. Y. Lam and B. Z. Tang, *Chem. Soc. Rev.*, 2011, **40**, 5361.

53 A. Qin, J. W. Y. Lam and B. Z. Tang, *Prog. Polym. Sci.*, 2012, **37**, 182.

54 Z. Zhao, J. W. Y. Lam and B. Z. Tang, *Curr. Org. Chem.*, 2010, **14**, 2109.

55 M. Wang, G. Zhang, D. Zhang, D. Zhu and B. Z. Tang, *J. Mater. Chem.*, 2010, **20**, 1858.

56 W. Qin, D. Ding, J. Liu, W. Z. Yuan, Y. Hu, B. Liu and B. Z. Tang, *Adv. Funct. Mater.*, 2012, **22**, 771.

57 H. Y. Chen, W. Y. Lam, J. D. Luo, Y. L. Ho, B. Z. Tang, D. B. Zhu, M. Wong and H. S. Kwok, *Appl. Phys. Lett.*, 2002, **81**, 574.

58 Z. Zhao, J. W. Y. Lam and B. Z. Tang, *J. Mater. Chem.*, 2012, **22**, 23726.

59 I. Javed, T. Zhou, F. Muhammad, J. Guo, H. Zhang and Y. Wang, *Langmuir*, 2012, **28**, 1439.

60 J. Chahine, N. Saffon, M. Cantuel and S. Fery-Forgues, *Langmuir*, 2011, **27**, 2844.

61 B. Xu, J. He, Y. Dong, F. Chen, W. Yu and W. Tian, *Chem. Commun.*, 2011, **47**, 6602.

62 S. Chen, Z. Zhao, B. Z. Tang and H.-S. Kwok, *Org. Electron.*, 2012, **13**, 1996.

63 T. Hirose, K. Higashiguchi and K. Matsuda, *Chem.–Asian J.*, 2011, **6**, 1057.

64 D.-M. Li and Y.-S. Zheng, *J. Org. Chem.*, 2011, **76**, 1100.

65 X. Huang, X. Gu, G. Zhang and D. Zhang, *Chem. Commun.*, 2012, **48**, 12195.

66 S. Chen, J. Liu, Y. Liu, H. Su, Y. Hong, C. K. W. Jim, R. T. K. Kwok, N. Zhao, W. Qin, J. W. Y. Lam, K. S. Wong and B. Z. Tang, *Chem. Sci.*, 2012, **3**, 1804.

67 X. Xu, J. Li, Q. Li, J. Huang, Y. Dong, Y. Hong, J. Yan, J. Qin, Z. Li and B. Z. Tang, *Chem.–Eur. J.*, 2012, **18**, 7278.

68 Q. Zhao, K. Li, S. Chen, A. Qin, D. Ding, S. Zhang, Y. Liu, B. Liu, J. Z. Sun and B. Z. Tang, *J. Mater. Chem.*, 2012, **22**, 15128.

69 Z. Zhao, J. W. Y. Lam, C. Y. K. Chan, S. Chen, J. Liu, P. Lu, M. Rodriguez, J.-L. Maldonado, G. Ramos-Ortiz, H. H. Y. Sung, I. D. Williams, H. Su, K. S. Wong, Y. Ma, H. S. Kwok, H. Qiu and B. Z. Tang, *Adv. Mater.*, 2011, **23**, 5430.

70 Z. Zhao, C. Y. K. Chan, S. Chen, C. Deng, J. W. Y. Lam, C. K. W. Jim, Y. Hong, P. Lu, Z. Chang, X. Chen, P. Lu, H. S. Kwok, H. Qiu and B. Z. Tang, *J. Mater. Chem.*, 2012, **22**, 4527.

71 Z. Zhao, S. Chen, X. Shen, F. Mahtab, Y. Yu, P. Lu, J. W. Y. Lam, H. S. Kwok and B. Z. Tang, *Chem. Commun.*, 2010, **46**, 686.

72 Y. Liu, J. W. Y. Lam, F. Mahtab, R. T. K. Kwok and B. Z. Tang, *Front. Chem. China*, 2010, **5**, 325.

73 W. Z. Yuan, F. Mahtab, Y. Gong, Z.-Q. Yu, P. Lu, Y. Tang, J. W. Y. Lam, C. Zhu and B. Z. Tang, *J. Mater. Chem.*, 2012, **22**, 10472.

74 Q. Chen, D. Zhang, G. Zhang, X. Yang, Y. Feng, Q. Fan and D. Zhu, *Adv. Funct. Mater.*, 2010, **20**, 3244.

75 Z. Zhao, Z. Wang, P. Lu, C. Y. K. Chan, D. Liu, J. W. Y. Lam, H. H. Y. Sung, I. D. Williams, Y. Ma and B. Z. Tang, *Angew. Chem., Int. Ed.*, 2009, **48**, 7608.

76 Z. Zhao, D. Liu, M. Faisal, L. Xin, Z. Shen, Y. Yu, C. Y. K. Chan, P. Lu, J. W. Y. Lam, H. H. Y. Sung, I. D. Williams, B. Yang, Y. Ma and B. Z. Tang, *Chem.–Eur. J.*, 2011, **17**, 5998.

77 J. Liu, H. Su, L. Meng, Y. Zhao, C. Deng, J. C. Y. Ng, P. Lu, M. Faisal, J. W. Y. Lam, X. Huang, H. Wu, K. S. Wong and B. Z. Tang, *Chem. Sci.*, 2012, **3**, 2737.

78 M. Wang, D. Zhang, G. Zhang and D. Zhu, *Chem. Phys. Lett.*, 2009, **475**, 64.

79 J.-H. Wan, L.-Y. Mao, Y.-B. Li, Z.-F. Li, H.-Y. Qiu, C. Wang and G.-Q. Lai, *Soft Matter*, 2010, **6**, 3195.

80 B.-K. An, S.-K. Kwon, S.-D. Jung and S. Y. Park, *J. Am. Chem. Soc.*, 2002, **124**, 14410.

81 B.-K. An, S. H. Gihm, J. W. Chung, C. R. Park, S.-K. Kwon and S. Y. Park, *J. Am. Chem. Soc.*, 2009, **131**, 3950.

82 S.-J. Yoon, J. H. Kim, J. W. Chung and S. Y. Park, *J. Mater. Chem.*, 2011, **21**, 18971.

83 B.-K. An, D.-S. Lee, J.-S. Lee, Y.-S. Park, H.-S. Song and S. Y. Park, *J. Am. Chem. Soc.*, 2004, **126**, 10232.

84 J. W. Chung, S.-J. Yoon, S.-J. Lim, B.-K. An and S. Y. Park, *Angew. Chem., Int. Ed.*, 2009, **48**, 7030.

85 J. Seo, J. W. Chung, E.-H. Jo and S. Y. Park, *Chem. Commun.*, 2008, 2794.

86 C. Bao, R. Lu, M. Jin, P. Xue, C. Tan, G. Liu and Y. Zhao, *Org. Biomol. Chem.*, 2005, **3**, 2508.

87 J. W. Chung, B. K. An and S. Y. Park, *Chem. Mater.*, 2008, **20**, 6750.

88 S. Qu, L. Zhao, Z. Yu, Z. Xiu, C. Zhao, P. Zhang, B. Long and M. Li, *Langmuir*, 2009, **25**, 1713.

89 S. Qu, L. Wang, X. Liu and M. Li, *Chem.–Eur. J.*, 2011, **17**, 3512.

90 S. Y. Ryu, S. Kim, J. Seo, Y.-W. Kim, O.-H. Kwon, D.-J. Jang and S. Y. Park, *Chem. Commun.*, 2004, 70.

91 A. Pérez, J. L. Serrano, T. Sierra, A. Ballesteros, D. de Saá and J. Barluenga, *J. Am. Chem. Soc.*, 2011, **133**, 8110.

92 X. Yang, R. Lu, T. Xu, P. Xue, X. Liu and Y. Zhao, *Chem. Commun.*, 2008, 453.

93 X. C. Yang, R. Lu, F. Y. Gai, P. C. Xue and Y. Zhan, *Chem. Commun.*, 2010, **46**, 1088.

94 D. Xu, X. Liu, R. Lu, P. Xue, X. Zhang, H. Zhou and J. Jia, *Org. Biomol. Chem.*, 2011, **9**, 1523.

95 T. H. Kim, M. S. Choi, B.-H. Sohn, S.-Y. Park, W. S. Lyoo and T. S. Lee, *Chem. Commun.*, 2008, 2364.

96 T. H. Kim, D. G. Kim, M. Lee and T. S. Lee, *Tetrahedron*, 2010, **66**, 1667.

97 Y. Qian, S. Li, Q. Wang, X. Sheng, S. Wu, S. Wang, J. Li and G. Yang, *Soft Matter*, 2012, **8**, 757.

98 M. K. Nayak, B.-H. Kim, J. E. Kwon, S. Park, J. Seo, J. W. Chung and S. Y. Park, *Chem.–Eur. J.*, 2010, **16**, 7437.

99 M. K. Nayak, *J. Photochem. Photobiol., A*, 2011, **217**, 40.

100 P. Xue, R. Lu, G. Chen, Y. Zhang, H. Nomoto, M. Takafuji and H. Ihara, *Chem.–Eur. J.*, 2007, **13**, 8231.